Photonic and Quantum Waves
https://www.sciltp.com/journals/pqw

Mini Review

Solitons in Optical Couplers: Introduction and Perspectives

Boris A. Malomed

Department of Physical Electronics, School of Electrical and Computer Engineering, Faculty of Engineering, Tel Aviv University, Tel Aviv 69978, Israel; malomed@tauex.tau.ac.il

How To Cite: Malomed, B.A. Solitons in Optical Couplers: Introduction and Perspectives. *Photonic and Quantum Waves* **2026**, *1*(1), 4. https://doi.org/10.53941/pqw.2026.100004

Received: 9 June 2026
Revised: 24 July 2026
Accepted: 3 August 2026
Published: 12 August 2026

Abstract: This minireview provides a brief summary and a discussion of directions for further development of theoretical and, chiefly, experimental studies of bright solitons in optical couplers, i.e., dual-core waveguides which combine the linear inter-core coupling (tunneling of light between parallel cores) with the intra-core group-velocity dispersion and self-focusing Kerr (cubic) nonlinearity. Following a short introduction to the field, the article focuses on a brief review of relatively recent experimental results for the switching of solitons in dual-core nonlinear optical fibers and the spontaneous emergence of stable asymmetric two-core solitons in the couplers with the symmetric dual-core structure.

Keywords: optical fibers; symmetry-breaking bifurcations; two-component solitons; soliton switching; soliton stability

1. Introduction

In the great variety of optical waveguides, one of basic types represents dual-core *couplers*, in which propagating optical waves tunnel between parallel guiding cores via evanescent fields penetrating the dielectric barrier separating the cores [1]. In most cases, the couplers are realized as twin-core optical fibers [2–4]. In a more sophisticated form, these may be inner twin-core structures in photonic-crystal fibers [5]. The dual-core fibers are fabricated by drawing an appropriately shaped preform from melt, or pressing together two single-mode fibers. Technology for the fabrication of a microstructured fiber with an inner dual guiding core is available too [6], see Figure 1.

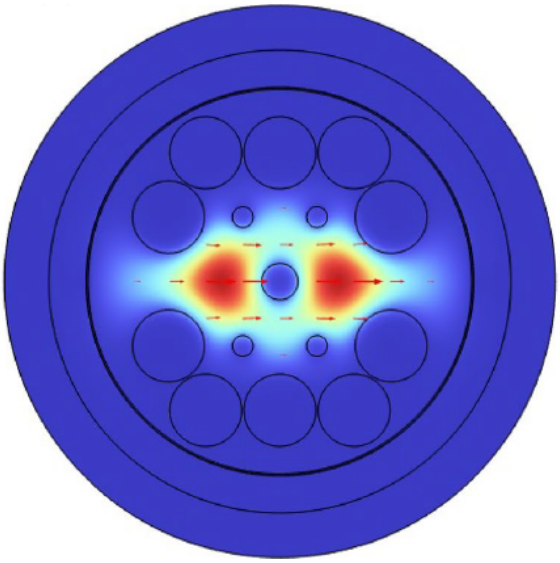

Figure 1. A schematic transverse profile of a microstructured optical fiber, with two tunnel-coupled waveguding cores created in it. Reprinted with permission from Ref. [7].

The wave exchange between the parallel cores in the coupler is affected by the intra-core nonlinearity [8,9]. This effect has been employed to design diverse all-optical switching devices [7,10–33] and other applications, such as

Copyright: © 2026 by the authors. This is an open access article under the terms and conditions of the Creative Commons Attribution (CC BY) license (https://creativecommons.org/licenses/by/4.0/).
Publisher's Note: Scilight stays neutral with regard to jurisdictional claims in published maps and institutional affiliations.

nonlinear amplifiers [17], logic gates [18], and bistability [20]. Nonlinear couplers can also provide efficient compression of solitons by transferring it into a fiber with a smaller value of the group-velocity dispersion (GVD) coefficient: the highest compression quality is achieved when two fibers with different GVD coefficients are not directly spliced one into the other, but are, instead, parallel-connected in the form of a coupler [19].

In addition to the basic dual-core system, the implementation of nonlinear couplers has been proposed in many other photonic settings, including light with the polarization structure [21], semiconductor waveguides [22], plasmonic media [23–25], twin-core fiber Bragg gratings [26,27], and others. In addition to the ubiquitous Kerr (cubic) nonlinearity of the core material, the analysis has been developed for systems with nonlinearities of other types, represented by saturable [28], quadratic (alias second-harmonic-generating) [29], cubic-quintic (CQ) [30], and nonlocal cubic terms [34]. Double-core transmission of light can be realized not only in optical fibers, but also in dual-core planar waveguides (i.e., in the *spatial domain*, rather than in the *temporal domain*) [25]. In most cases, the nonlinear dual-core waveguides are adequately modeled by systems of linearly coupled nonlinear Schrödinger equations (NLSEs), in which the tunneling of light between the cores is accounted for by linear-coupling terms [8,9,35,36]. The coupler concept was also extended for the *spatiotemporal* propagation of light in dual-core planar waveguides, with the respective one-dimensional NLSE system replaced by its two-dimensional version, which includes the temporal and spatial coordinates [37].

A fundamental property of nonlinear couplers with mutually symmetric twin cores is the *symmetry-breaking bifurcation* (SBB), which destabilizes obvious symmetric modes and gives rise to asymmetric ones. The SBB was first analyzed for uniform states (alias continuous waves, CWs) in dual-core nonlinear optical fibers [35], and then for solitons in the same system [36,38–41], as well as for dual-core nonlinear fibers with Bragg gratings (BGs) written on each core [26]. Some theoretical results on this topic were summarized in an early review [42], and later in Ref. [43]. The SBB analysis was then extended to solitons in couplers with the quadratic [29] and CQ [30] nonlinearities.

The cubic (Kerr) nonlinearity in the dual-core system gives rise to the *subcritical* SBB for solitons. This means that it originally produces unstable branches of asymmetric modes which evolve *backward* in the parameter plane of the soliton's energy and asymmetry degree (in the direction of smaller energy. i.e., weaker nonlinearity), see Figure 2. Then, the branches turn forward, retrieving stability at the turning points (the bold ones in Figure 2) [44]. On the other hand, the *supercritical* SBB immediately gives rise to stable branches of asymmetric solitons, which evolve strictly in the forward direction. For solitons in couplers, the SBB of the latter type occurs in twin-core BGs [26], and in the system with the quadratic nonlinearity [29].

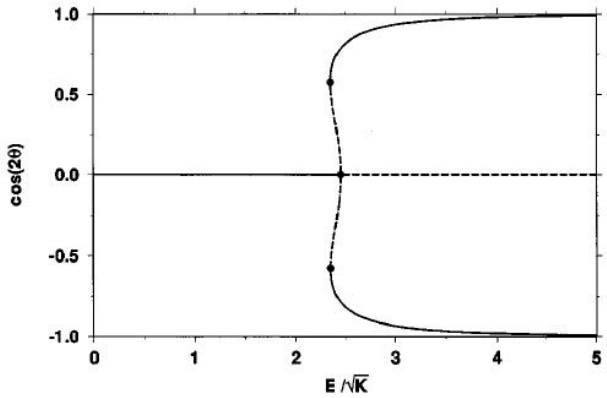

Figure 2. The dependence of the asymmetry parameter $\cos(2\theta)$ of the two-component solitons (see Equation (12)), in the nonlinear coupler with identical cores, on the scaled total energy, $E/\sqrt{K}$, as predicted by the VA, see Equation (12). The figure demonstrates a weakly subcritical SBB, solid and dashed lines designating stable and unstable states, respectively. Reprinted with permission from Ref. [41].

In the model of the dual-core coupler with the cubic intra-core nonlinearity, the SBB point for symmetric solitons was found in an exact analytical form [36]. The asymmetric solitons emerging at the SBB point were studied analytically by means of the variational approximation (VA) [26,28,29,37,38] and in the numerical form [45,46] (in addition to the original works which reported these findings, see also a summary in reviews [4,42,43]).

While the theoretical analysis of solitons in dual-core optical systems was elaborated in detail, starting in 1989 [36,38–41,45,46], the first experimental realization of this phenomenology in optical fibers was reported only in 2020 [16], which initiated renewed interest to this topic and stimulated further experimental studies [31–33]. The objective of the present mini-review is to briefly summarize the experimental findings for the solitons, as a topic with considerable potential for further work. Because these findings are relatively novel ones, they were not included in

the previous reviews on the theme of solitons in dual-core systems [4,42,43].

The subsequent presentation is organized as follows. First, a necessary summary of well-known theoretical results, which are focused on the prediction of the SBB in nonlinear fiber-optic couplers, is presented in a brief form in Section 3. This is followed by the core part of the article, *viz.*, the summary of the relatively recent experimental findings for the solitons. The article is concluded by Section 4.

2. Solitons in Dual-Core Nonlinear Fibers: The Basic (Well-Established) Theory

The basic model of the symmetric coupler amounts to the system of linearly coupled NLSEs [3]:

$$iu_z + \frac{1}{2}u_{\tau\tau} + |u|^2 u + Kv = 0, \tag{1}$$

$$iv_z + \frac{1}{2}v_{\tau\tau} + |v|^2 v + Ku = 0. \tag{2}$$

Here z is the propagation distance, $\tau \equiv t - z/V_{\rm gr}$ is the reduced time (t is the physical time, and $V_{\rm gr}$ is the group velocity of the carrier wave [47]), u and v are envelopes of the optical waves in the coupled cores, the second derivatives represent the anomalous GVD [47], the cubic terms represent the Kerr nonlinearity in the cores, and real K is the coupling constant accounting for the tunneling of light between the cores, which may always be defined to be positive.

Equations (1) and (2) can be derived from the respective Lagrangian (L), which is a combination of the kinetic terms and the Hamiltonian (H) [43]:

$$L = \int_{-\infty}^{+\infty} \left[\frac{i}{2}\left(u^* u_z + v^* v_z\right) d\tau + \text{c.c.} \right] - H, \tag{3}$$

$$H = \int_{-\infty}^{+\infty} \left[\frac{1}{2}\left(|u_\tau|^2 + |v_\tau|^2\right) - \frac{1}{2}\left(|u|^4 + |v|^4\right) - K\left(u^* v + u v^*\right) \right], \tag{4}$$

where both the asterisk and c.c. stand for the complex conjugate. The Hamiltonian, along with the energy (alias the total norm) of the solution,

$$E = \frac{1}{2}\int_{-\infty}^{+\infty} \left(|u|^2 + |v|^2\right) d\tau \equiv E_u + E_v, \tag{5}$$

and the total momentum,

$$P = \frac{i}{2}\int_{-\infty}^{+\infty} \left[\left(u u_\tau^* + v v_\tau^*\right) + \text{c.c.}\right] d\tau, \tag{6}$$

are dynamical invariants of the system. Note that the energy is different from the Hamiltonian, in the present context.

Equations (1) and (2) admit obvious symmetric and antisymmetric soliton solutions,

$$u = \pm v = T^{-1}\text{sech}\left(\frac{\tau}{T}\right)\exp\left(\frac{iz}{2T^2} \pm iKz\right), \tag{7}$$

where T is the temporal width of the soliton, which determines its energy and Hamiltonian:

$$E_\pm = 2T^{-1},\ H_\pm = -\frac{2}{3}T^{-3} \mp 4KT^{-1}. \tag{8}$$

The antisymmetric solitons make the coupling term in Hamiltonian (8) positive, unlike the negative one for the symmetric states. For this reason, the antisymmetric solitons always correspond to a maximum, rather than minimum, of the Hamiltonian, which makes them always unstable [46]. Therefore, the antisymmetric modes are not considered below.

The issue of major interest is the SBB, which destabilizes the symmetric solitons and creates stable asymmetric ones, with unequal energies of their components, but still identical signs of the corresponding wave fields, inherited from the symmetric states. The value of the energy of the symmetric soliton at the SBB point is known in an exact form [36]:

$$E = E_{\rm bif} \equiv 4\sqrt{K/3} \approx 2.31\sqrt{K}. \tag{9}$$

Asymmetric solitons, which emerge at the SBB point, cannot be found in an exact analytical form, but they can be studied by means of VA [38–41]. This approximation is based on the following trial analytical form (*ansatz*) for the two-component soliton solution of Equations (1) and (2):

$$u = A\cos(\theta)\mathrm{sech}\left(\frac{\tau}{T}\right)\exp\left(i(\phi+\psi)+ib\tau^2\right), \tag{10}$$

$$v = A\sin(\theta)\mathrm{sech}\left(\frac{\tau}{T}\right)\exp\left(i(\phi-\psi)+ib\tau^2\right), \tag{11}$$

where the real shape parameters A and T are the overall amplitude and temporal width of the soliton, while real θ, provided that it takes values $\neq \pi/4$, determines the asymmetry between the components, in terms of the relative difference of their energies (see Equation (5)),

$$\cos(2\theta) \equiv \frac{E_u - E_v}{E_u + E_v}. \tag{12}$$

Further, $\phi(z)$ and $\psi(z)$ are, respectively, overall and relative phases of the two-component soliton, while real *chirp* $b(z)$ must be introduced if the ansatz admits variation of the width as a function of z [48,49]. The asymmetric solitons with $E_u > E_v$ and $E_u < E_v$, i.e., $\theta > \pi/4$ and $\theta < \pi/4$, respectively (see Equation (12)), may be considered as the asymmetric modes with *opposite polarities*.

Switching of a soliton between the two cores of the coupler was considered, in the framework of a full system of variational equations for ansatz (10) and (11) in Ref. [50]. For static solitons, ansatz (10) and (11) with $b = 0$ gives rise to the following variational equations, in which all parameters of ansatz (10) and (11), except for the phase $\phi(z)$, are assumed constant:

$$\sin(2\theta)\sin(2\psi) = 0, \tag{13}$$

$$\frac{E}{3T}\cos(2\theta) - K\cot(2\theta)\cos(2\psi) = 0, \tag{14}$$

$$T^{-1} = E\left[1 - \frac{1}{2}\sin^2(2\theta)\right], \tag{15}$$

$$\frac{d\phi}{dz} = -\frac{1}{6T^2} + \frac{2E}{3T}\left(1 - \frac{1}{2}\sin^2(2\theta)\right) + \kappa\sin(2\theta)\cos(2\psi).$$

Here E is the soliton's total energy, which, according to its definition (5), takes value $E = A^2T$ for ansatz (10) and (11).

As it follows from Equation (13), the static asymmetric soliton, i.e., one with $\theta \neq \pi/4$ (see Equation (12)), has $\sin(2\psi) = 0$, which implies that $\cos(2\psi) = \pm 1$. As mentioned above, the solutions corresponding to $\cos(2\psi) = -1$, i.e., antisymmetric ones, with respect to the two components, are unstable. Therefore, only the case of $\cos(2\psi) = +1$, corresponding to solitons with in-phase components ($\psi = 0$), is relevant. Then, the soliton's width T can be eliminated by means of Equation (15), and the remaining Equation (15) for the energy-distribution angle θ takes the form of

$$\cos(2\theta)\left[\frac{E^2}{3K}\sin(2\theta)\left(1 - \frac{1}{2}\sin^2(2\theta)\right) - 1\right] = 0. \tag{16}$$

Further analysis reveals that, in the interval $0 < E < E_1$, where

$$E_1 = \sqrt{(9/4)\sqrt{6}K} \approx 2.348\sqrt{K}, \tag{17}$$

the only relevant solution to Equation (16) is the symmetric one, with $\theta = \pi/4$ and equal energies in both components, according to Equations (10)–(12). When the soliton's energy attains value E_1, predicted by Equation (17), *asymmetric* solutions emerge by a jump from $\cos(2\theta) = 0$ to

$$\cos(2\theta) = \pm 1/\sqrt{3}. \tag{18}$$

When E attains a slightly larger value,

$$E_2 = \sqrt{6K} \approx 2.450\sqrt{K}, \tag{19}$$

the above-mentioned *backward (subcritical) bifurcation* [44] occurs, which makes the symmetric solution with $\theta = \pi/4$ unstable. The (slightly) subcritical character of the bifurcation, with respect to the variation of energy E, is confirmed by the fact that the asymmetric soliton (18) appears at the energy value (17) which is *slightly smaller* than the value of E at the bifurcation point (19). The comparison with the full numerical results corroborates the weakly subcritical shape of the SBB for solitons in the nonlinear coupler [41].

A typical example of the asymmetric soliton is displayed in Figure 3, and the SBB diagram is presented in Figure 2. One can easily distinguish between stable and unstable branches in the diagram, using elementary theorems

of the bifurcation theory [44]. Note also that the emergence of the pairs of stable and unstable asymmetric solitons "from nothing" at points (17), which are denoted by the bold dots in Figure 2, is an elementary bifurcation of another type, known as the *saddle-node* bifurcation [44].

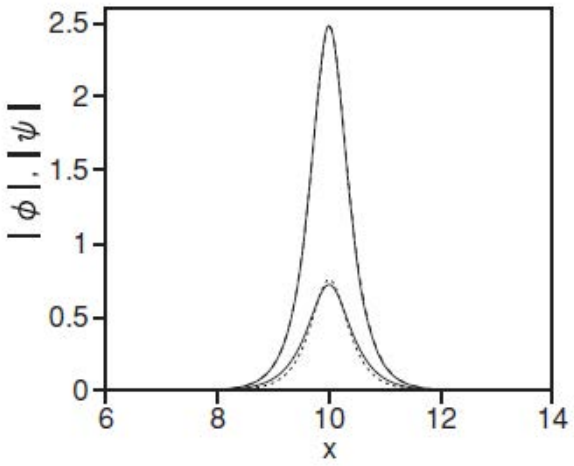

Figure 3. A typical example of two components of a stable asymmetric soliton, with $|\phi(x)| \equiv U(\tau)$, $|\psi(x)| \equiv V(\tau)$. Continuous and dashed lines designate the numerically found solution and its VA-produced counterpart, respectively. Reprinted with permission from Ref. [51].

Thus, the VA predicts that the backward (subcritical) bifurcation occurs at the value of the soliton's energy given by Equation (19). The accuracy of the VA is characterized by comparison of this prediction with the above-mentioned exact bifurcation value (9), the relative error being 0.057.

The above consideration addressed a single soliton in the nonlinear coupler. A cruder version of the VA was used to analyze two-soliton interactions in the same system [52]. Accurate numerical results for the interactions were reported in [53]. Furthermore, it was also demonstrated that chains of stable solitons with alternating signs in the dual-core fiber support the propagation of *supersolitons*, i.e., localized collective excitations in the chain of solitons [54]. The underlying chain may be built of symmetric solitons, as well as of asymmetric ones with *alternating polarities*, i.e., intermittent placements of larger and smaller components in the two cores.

3. Solitons in Dual-Core Fibers: Experimental Results and the Theoretical Framework

As said above, the experimental observation of solitons in nonlinear optical couplers was reported much later than such solitons were predicted theoretically. The spontaneous formation of asymmetric temporal solitons in the symmetric dual-core fiber was first experimentally demonstrated using a sample of length 4.3 cm, with the anomalous-GVD coefficient in each core $\beta_2 = -0.0773$ ps^2/m in physical units [16]. The sample was fabricated in a drawing tower, using an optimally designed preform. The coupler's switching length, i.e., a characteristic propagation length necessary for the transfer of an optical signal between the cores, in the linear regime (this propagation distance is defined as $1/K$, in terms of Equations (1) and (2)), was 1.3 cm.

In the experiment, soliton-like pulses of temporal length 75 fs, carried by the standard telecommunication wavelength, 1560 nm, were coupled into one core of the double fiber at repetition rate 100 MHz, while the other core was left initially empty. In terms of Equations (1) and (2), this input is modeled by the initial conditions

$$u(\tau, z = 0) = a \operatorname{sech}(\eta\tau), u(\tau, z = 0) = 0, \tag{20}$$

with amplitude a and temporal width $1/\eta$. The energy of the input pulses was varied, in physical units, in the range of 50–250 pJ. The results were observed in the form of the transverse intensity distribution in the output, which was recorded as a camera image in the fiber facet (including both cores).

Before displaying the experimental results, it is relevant to produce the theoretical prediction, provided by simulations of Equations (1) and (2) with initial conditions (20). At relatively low values of the energy, which is $E = 2a^2\eta^{-1}$ in terms of input (20), when the stationary solution gives rise to the stable symmetric soliton (see Figure 3)), the full numerical simulations produce a soliton-like pulse periodically oscillating between the two cores, as shown in the top-row panels in Figure 4. Similar experimental results for periodic switching of temporal optical pulses between the cores were reported in work [31], for the carrier wavelength 1700 nm and a higher energy scale. The increase of the energy leads to a transition from the oscillatory regime to a quasi-stationary state, in which

the soliton has once switched from the input (*straight*) core into the second (*cross*) one, where it self-traps into an asymmetric soliton, with a smaller residual component remaining in the straight core. This outcome is demonstrated by accurate simulations in the central row of panels in Figure 4. Finally, at the largest considered values of energy, the strong nonlinearity keeps the input pulse in the straight core, where it directly self-traps into the corresponding strongly asymmetric soliton. The latter outcome of the evolution of the input pulse is shown by accurate simulations in the bottom row of panels in Figure 4.

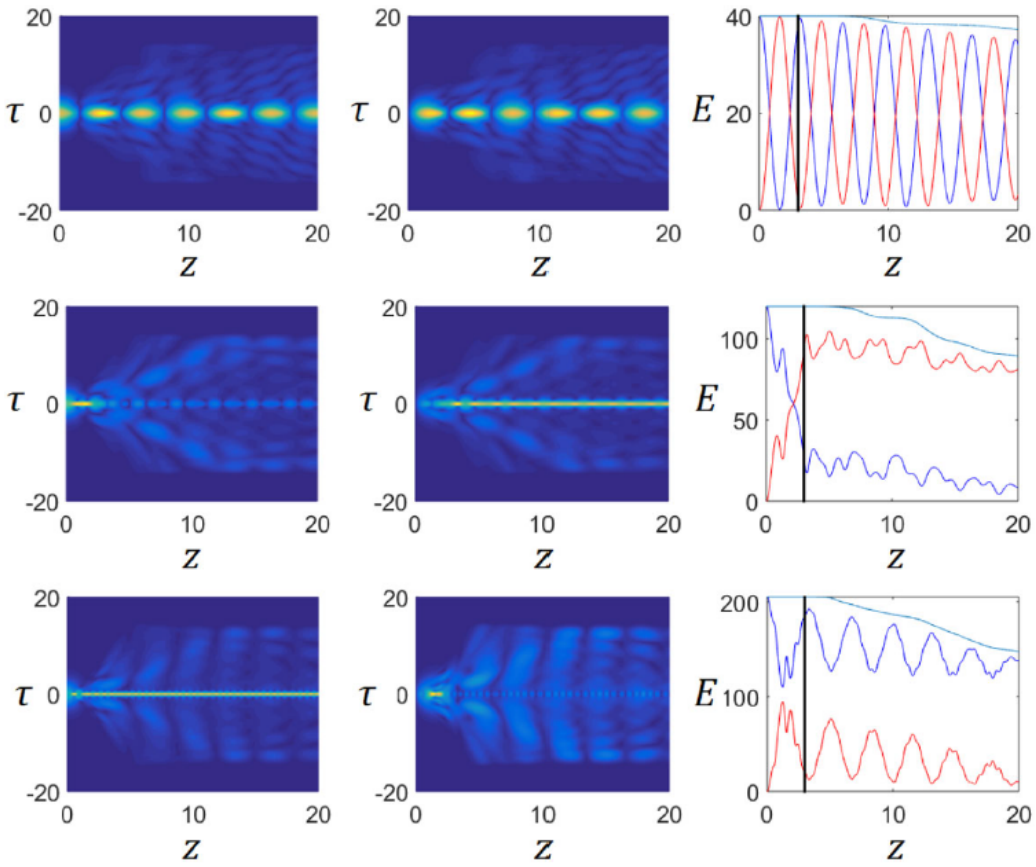

Figure 4. Switching between the coupler's cores, produced by simulations of Equations (1) and (2) with initial conditions (20), for three values of the input amplitude, $a = 1.15$, 2.0, 2.6 (from top to bottom), and a fixed inverse width, $\eta = 0.78$. The left and central columns display spatiotemporal patterns of the intensities, $|u(z,\tau)|^2$ and $|v(z,\tau)|^2$, in the straight and cross cores, respectively. The blue and red curves in the right column show the energy in each channel (and the total energy, shown by the cyan curve) vs. the propagation distance. The top, central, and bottom panels represent, severally, regimes with periodic inter-core oscillations, switching into the cross core followed by the self-trapping of the asymmetric soliton in it, and the immediate self-trapping of the asymmetric soliton in the straight core, respectively. The vertical line at $z = 3$ denotes the fiber length in the experiment. The picture is plotted in scaled units. Reprinted with permission from Ref. [16].

The theoretically predicted transitions between the different propagation outcomes which are displayed in Figure 4, including the self-trapping of the asymmetric solitons, were directly observed in the experiments reported in work [16], as shown in Figure 5. Systematic analysis of the experimental data produces a general conclusion: for the above-mentioned fixed value of the temporal width of input (20), 75 fs (in physical units), the gradual increase of the input's energy E yields the periodic inter-core oscillations, self-trapping of the asymmetric soliton in the cross core, and, eventually, self-trapping of the strongly asymmetric soliton in the straight core, in the energy intervals of 50–100 pJ, 100–150 pJ, and 150–250 pJ, respectively (in physical units too). In particular, the output patterns presented in Figure 5 for $E = 50$ pJ and 100 pJ (in the regime of relatively weak nonlinearity) correspond to the oscillatory regime. In this case, the energy distribution between the cores in the output returns, approximately, to the input state (cf. the top row in the theoretically produced plot displayed in Figure 4). In the regime of intermediately strong nonlinearity, the experimentally observed output, shown in Figure 5 for $E = 150$ pJ, corresponds to the transition from the periodic oscillations to the self-trapping of the asymmetric soliton in the cross core with residual oscillations (the length of the fiber is not sufficient to achieve the fully self-trapped state in this case, similar to what

is observed in the simulations which are displayed in the mid row of Figure 4). Finally, in the strongly nonlinear regime, the experimentally observed outputs for $E = 200$ pJ and 250 pJ, which are also displayed in Figure 5, represent the strongly asymmetric solitons with residual oscillations, which have self-trapped directly in the straight core, cf. the bottom row in the theoretical simulations displayed in Figure 4. Similar experimental results were also observed at other values of parameters, such as the temporal width of the input.

Some differences between the experimental findings and predictions produced by the simulations of Equations (1) and (2) are explained by effects of the third-order dispersion and the Raman self-frequency shift for the optical pulses, which are not included in the theoretical model.

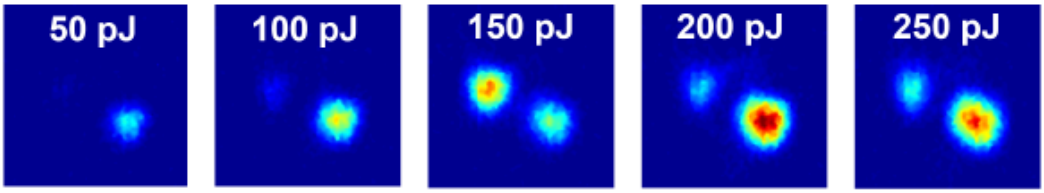

Figure 5. A sequence of camera images of the output intensity patterns, taken in the fiber facet, for different energies of the input and its fixed temporal width, 75 fs. Reprinted with permission from Ref. [16].

The findings summarized here and shown in Figure 5 provide the first experimental observation of the asymmetric solitons in the symmetric nonlinear optical coupler, which was theoretically predicted more than twenty years earlier [36,38–41,45,46], see also the review [4]. The demonstration of theoretically predicted sophisticated features of the symmetry-breaking phenomenology, such as weakly subcritical character of the SBB, expected according to Figure 2, makes it necessary to perform the experimental studies with a very high accuracy. It is also relevant to mention other theoretically explored situations which call for the continuation of the experimental work in various directions, such as collisions between bright and dark solitons in optical couplers [53], higher-order bright solitons (breathers), etc.

Solitons in asymmetric dual-core optical fibers have been experimentally created as well [32, 33]. Those solitons have a natural asymmetric structure,

4. Conclusions

Dual-core optical fibers is a research area which gives rise to a great variety of topics for fundamental theoretical and experimental studies, as well as a plenty of existing and potentially possible applications in optics, photonics, and plasmonics. While currently employed devices based on dual-core optical waveguides operate in the linear regime (couplers, splitters, etc.), the use of the intrinsic nonlinearity offers many options, chiefly related to the use of self-trapped robust modes in the form of solitons. In particular, they may be used as data bits in all-optical integrated schemes of information processing. Then, the dynamical effects offered by the dual-core waveguides, such as the self-trapping of solitons in a particular core and switch between the cores, can be employed for the design of setups controlling the data flow.

In terms of fundamental studies, solitons in dual-core fibers are the subject of dominant interest, as they offer a setting for the implementation of many static and dynamical phenomena based on solitons. Furthermore, optical solitons in dual-core fibers may be used to emulate soliton phenomenology in other fields of physics, such as Bose-Einstein condensates.

Theoretical studies of solitons in these systems had begun about four decades ago [3,10–12,21,35,36,38–40,42,45,46]. While the basic part of the theoretical analysis has been essentially completed, there remain many directions for the extension of the studies. In particular, a natural generalization of dual-core fibers is provided by multi-core arrays, which allow the creation of self-trapped modes that are discrete and continuous ones, in the directions across and along the array, respectively. These modes include *semi-discrete solitons*, which may be created in many settings [55–59]. Another generalization implies the transition from 1D to 2D couplers, represented by dual-core planar optical waveguides. The consideration of the spatiotemporal propagation in these system makes it possible to predict the existence of novel species of 2D stable "light bullets" (spatiotemporal solitons [60]), including *spatiotemporal vortices* [37].

From many theoretical predictions, only few ones have been realized experimentally. A brief survey of the experimental results and an outline of perspectives for the development of the experimental work in this field, which was not reviewed previously, is the main subject of the present article. In particular, the fundamentally important species of the asymmetric solitons in symmetric dual-core fibers, which were predicted long ago [36, 38–41], have been reported in the experiment much later [16]. Another noteworthy experimental result is the creation of

semi-discrete "light bullets" [61], including ones with embedded vorticity [62] (actually, in a transient form), in three-dimensional arrays of fiber-like waveguides permanently written in bulk samples of silica. Thus, further development of experimental studies in this vast area remains a highly relevant objective.

Funding

This research received no external funding.

Institutional Review Board Statement

Not applicable.

Informed Consent Statement

Not applicable.

Data Availability Statement

Not applicable.

Acknowledgments

I thank colleagues with whom I have had a chance to collaborate on the theoretical and experimental topics considered in this article: L. Albuch, J. Atai, R. Blit, I. Bugar, R. Buzcynski, K. S. Chiang, N. Dror, N. V. Hung, Y. S. Kivshar, F. Lederer, L. Li, P. Li, M. Longobucco, W. C. K. Mak, V. H. Nguyen, G. D. Peng, H. Sakaguchi, I. M. Skinner, L. X. T. Tai, R. Tasgal, M. Trippenbach, I. M. Uzunov, and F. Ye.

Conflicts of Interest

Given the role as Editor-in-Chief, Boris A. Malomed had no involvement in the peer review of this paper and had no access to information regarding its peer-review process. Full responsibility for the editorial process of this paper was delegated to another editor of the journal.

Use of AI and AI-Assisted Technologies

No AI tools were utilized for this paper.

References

1. Huang, W.P. Coupled-mode theory for optical waveguides: An overview. *J. Opt. Soc. Am. A* **1994**, *11*, 963–983.
2. Digonnet, M.J.F.; Shaw, H.J. Analysis of a tunable single-mode optical fiber coupler. *IEEE J. Quantum Electron.* **1982**, *18*, 746–754.
3. Trillo, S.; Wabnitz, S.; Wright, E.M.; et al. Soliton switching in fiber nonlinear directional couplers. *Opt. Lett.* **1988**, *13*, 672–674.
4. Malomed, B.A. A variety of dynamical settings in dual-core nonlinear fibers. In *Handbook of Optical Fibers*, Vol. 1; Peng, G.-D., Ed.; Springer: Singapore, 2019; pp. 421–474.
5. Saitoh, K.; Sato, Y.; Koshiba, M. Coupling characteristics of dual-core photonic crystal fiber couplers. *Opt. Express* **2003**, *11*, 3188–3195.
6. MacPherson, W.N.; Jones, J.D.C.; Mangan, B.J.; et al. Two-core photonic crystal fibre for Doppler difference velocimetry. *Opt. Commun.* **2003**, *223*, 375–380.
7. Maurya, V.C.; Trabelsi, Y.F.; Varshney, A.D.; et al. Ultra-sensitive graphene–gold hybrid dual core photonic crystal fiber sensor based on surface plasmon resonance for bio-analyte detection. *Sci. Rep.* **2026**, *16*, 8478.
8. Jensen, S.M. The nonlinear coherent coupler. *IEEE J. Quantum Electron.* **1982**, *18*, 1580–1583.
9. Maier, A.A. Optical transistors and bistable devices utilizing nonlinear transmission of light in systems with unidirectional coupled waves. *Sov. J. Quantum Electron.* **1982**, *12*, 1490–1494.
10. Friberg, S.R.; Silberberg, Y.; Oliver, M.K.; et al. Ultrafast all-optical switching in dual-core fiber nonlinear coupler. *Appl. Phys. Lett.* **1987**, *51*, 1135–1137.
11. Friberg, S.R.; Weiner, A.M.; Silberberg, Y.; et al. Femtosecond switching in dual-core-fiber nonlinear coupler. *Opt. Lett.* **1988**, *13*, 904–906.
12. Heatley, D.R.; Wright, E.M.; Stegeman, G.I. Soliton coupler. *Appl. Phys. Lett.* **1988**, *53*, 172–174.
13. Królikowski, W.; Kivshar, Y.S. Soliton-based optical switching in waveguide arrays. *J. Opt. Soc. Am. B* **1996**, *13*, 876–887.
14. Tsang, S.C.; Chiang, K.S.; Chow, K.W. Soliton interaction in a two-core optical fiber. *Opt. Commun.* **2004**, *229*, 431–439.
15. Lederer, F.; Stegeman, G.I.; Christodoulides, D.N.; et al. Discrete solitons in optics. *Phys. Rep.* **2008**, *463*, 1–126.

16. Nguyen, V.H.; Tai, L.X.T.; Bugar, I.; et al. Reversible ultrafast soliton switching in dual-core highly nonlinear optical fibers. *Opt. Lett.* **2020**, *45*, 5221–5224.
17. Malomed, B.A.; Peng, G.D.; Chu, P.L. A nonlinear optical amplifier based on a dual-core fiber. *Opt. Lett.* **1996**, *21*, 330–332.
18. Wu, Y.D. Coupled-soliton all-optical logic device with two parallel tapered waveguides. *Fiber Integr. Opt.* **2004**, *23*, 405–414.
19. Hatami-Hanza, H.; Chu, P.L.; Malomed, B.A.; et al. Soliton compression and splitting in double-core nonlinear optical fibers. *Opt. Commun.* **1997**, *134*, 59–65.
20. Chevriaux, D.; Khomeriki, R.; Leon, J. Bistable transmitting nonlinear directional couplers. *Mod. Phys. Lett. B* **2006**, *20*, 515–532.
21. Trillo, S.; Wabnitz, S. Coupling instability and power-induced switching with 2-core dual-polarization fiber nonlinear coupler. *J. Opt. Soc. Am. B* **1988**, *5*, 483–491.
22. Villeneuve, A.; Yang, C.C.; Wigley, P.C.J.; et al. Ultrafast all-optical switching in semiconductor nonlinear directional couplers at half the band-gap. *Appl. Phys. Lett.* **1992**, *61*, 147–149.
23. Hochberg, M.; Baehr-Jones, T.; Walker, C.; et al. Integrated plasmon and dielectric waveguides. *Opt. Express* **2004**, *12*, 5481–5486.
24. Petráček, J. Nonlinear directional coupling between plasmonic slot waveguides. *Appl. Phys. B* **2013**, *112*, 593–598.
25. Smirnova, D.A.; Gorbach, A.V.; Iorsh, I.V.; et al. Nonlinear switching with a graphene coupler. *Phys. Rev. B* **2013**, *88*, 045443.
26. Mak, W.C.K.; Malomed, B.A.; Chu, P.L. Solitary waves in coupled nonlinear waveguides with Bragg gratings. *J. Opt. Soc. Am. B* **1998**, *15*, 1685–1692.
27. Sun, Y.; White, T.P.; Sukhorukov, A.A. Coupled-mode theory analysis of optical forces between longitudinally shifted periodic waveguides. *J. Opt. Soc. Am. B* **2013**, *30*, 736–742.
28. Peng, G.D.; Chu, P.L.; Ankiewicz, A. Soliton propagation in saturable nonlinear fiber couplers–variational and numerical results. *J. Nonlinear Opt. Phys. Mater.* **1994**, *3*, 69–87.
29. Mak, W.C.K.; Malomed, B.A.; Chu, P.L. Soliton coupling in waveguide with quadratic nonlinearity. *Phys. Rev. E* **1997**, *55*, 6134–6140.
30. Albuch, L.; Malomed, B.A. Transitions between symmetric and asymmetric solitons in dual-core systems with cubic-quintic nonlinearity. *Math. Comput. Simul.* **2007**, *74*, 312–322.
31. Longobucco, M.; Astrauskas, I.; Pugžlys, A.; et al. Broadband self-switching of femtosecond pulses in highly nonlinear high index contrast dual-core fibre. *Opt. Commun.* **2020**, *472*, 126043.
32. Nguyen, V.H.; Longobucco, M.; Buczyński, R.; et al. Self-trapping and switching of solitonic pulses in mismatched dual-core highly nonlinear fibers. *Chaos Solitons Fractals* **2023**, *167*, 113045.
33. Tai, L.X.T.; Longobucco, M.; Hung, N.V.; et al. Analysis of high-contrast all-optical dual wavelength switching in asymmetric dual-core fibers. *Opt. Lett.* **2024**, *49*, 149–152.
34. Shi, X.; Malomed, B.A.; Ye, F.; et al. Symmetric and asymmetric solitons in a nonlocal nonlinear coupler. *Phys. Rev. A* **2012**, *85*, 053839.
35. Snyder, A.W.; Mitchell, D.J.; Poladian, L.; et al. Physics of nonlinear fiber couplers. *J. Opt. Soc. Am. B* **1991**, *8*, 2102–2112.
36. Wright, E.M.; Stegeman, G.I.; Wabnitz, S. Solitary-wave decay and symmetry-breaking instabilities in two-mode fibers. *Phys. Rev. A* **1989**, *40*, 4455–4466.
37. Dror, N.; Malomed, B.A. Symmetric and asymmetric solitons and vortices in linearly coupled two-dimensional waveguides with the cubic-quintic nonlinearity. *Physica D* **2011**, *240*, 526–541.
38. Paré, C.; Florjańczyk, M. Approximate model of soliton dynamics in all-optical fibers. *Phys. Rev. A* **1990**, *41*, 6287–6295.
39. Maimistov, A.I. Propagation of a light pulse in nonlinear tunnel-coupled optical waveguides. *Sov. J. Quantum Electron.* **1991**, *21*, 687–690.
40. Chu, P.L.; Malomed, B.A.; Peng, G.D. Soliton switching and propagation in nonlinear fiber couplers: Analytical results. *J. Opt. Soc. Am. B* **1993**, *10*, 1379–1385.
41. Malomed, B.A.; Skinner, I.M.; Chu, P.L.; et al. Symmetric and asymmetric solitons in twin-core nonlinear optical fibers. *Phys. Rev. E* **1996**, *53*, 4084–4091.
42. Romagnoli, M.; Trillo, S.; Wabnitz, S. Soliton switching in nonlinear couplers. *Opt. Quantum Electron.* **1992**, *24*, S1237–S1267.
43. Malomed, B.A. Variational methods in fiber optics and related fields. In *Progress in Optics*, Vol. 43; Wolf, E., Ed.; North-Holland: Amsterdam, Netherlands, 2002; pp. 71–193.
44. Iooss, G.; Joseph, D.D. *Elementary Stability and Bifurcation Theory*; Springer: Berlin, Germany, 1980.
45. Akhmediev, N.; Ankiewicz, A. Novel soliton states and bifurcation phenomena in nonlinear fiber couplers. *Phys. Rev. Lett.* **1993**, *70*, 2395–2398.
46. Soto-Crespo, J.M.; Akhmediev, N. Stability of the soliton states in a nonlinear fiber coupler. *Phys. Rev. E* **1993**, *48*, 4710–4715.
47. Agrawal, G.P. *Nonlinear Fiber Optics*, Fourth edition; Academic Press: San Diego, CA, USA, 2007.
48. Anderson, D. Variational approach to nonlinear pulse propagation in optical fibers. *Phys. Rev. A* **1983**, *27*, 3135–3145.
49. Anderson, D.; Lisak, M.; Reichel, T. Asymptotic propagation properties of pulses in a soliton-based optical-fiber

communication system. *J. Opt. Soc. Am. B* **1988**, *5*, 207–210.
50. Uzunov, I.M.; Muschall, R.; Gölles, M.; et al. Pulse switching in nonlinear fiber directional couplers. *Phys. Rev. E* **1995**, *51*, 2527–2537.
51. Sakaguchi, H.; Malomed, B.A. Symmetry breaking of solitons in two-component Gross-Pitaevskii equations. *Phys. Rev. E* **2011**, *83*, 036608.
52. Doty, S.L.; Haus, J.W.; Oh, Y.; et al. Soliton interactions on dual-core fibers. *Phys. Rev. E* **1995**, *51*, 709–717.
53. Peng, G.D.; Malomed, B.A.; Chu, P.L. Soliton collisions in a model of a dual-core nonlinear optical fiber. *Phys. Scr.* **1998**, *58*, 149–158.
54. Li, P.; Li, L.; Malomed, B.A. Multisoliton Newton's cradles and supersolitons in regular and parity-time-symmetric nonlinear couplers. *Phys. Rev. E* **2014**, *89*, 062926.
55. Aceves, A.B.; De Angelis, C.; Rubenchik, A.M.; et al. Multidimensional solitons in fiber arrays. *Opt. Lett.* **1994**, *19*, 329–331.
56. Aceves, A.B.; De Angelis, C.; Luther, G.G.; et al. Modulational instability of continuous waves and one-dimensional temporal solitons in fiber arrays. *Opt. Lett.* **1994**, *19*, 1186–1188.
57. Aceves, A.B.; Luther, G.G.; De Angelis, C.; et al. Energy localization in nonlinear fiber arrays: Collapse-effect compressor. *Phys. Rev. Lett.* **1995**, *75*, 73–76.
58. Matsumoto, M.; Katayama, S.; Hasegawa, A. Optical switching in nonlinear waveguide arrays with a longitudinally decreasing coupling coefficient. *Opt. Lett.* **1995**, *20*, 1758–1760.
59. Blit, R.; Malomed, B.A. Propagation and collisions of semidiscrete solitons in arrayed and stacked waveguides. *Phys. Rev. A* **2012**, *86*, 043841.
60. Silberberg, Y. Collapse of optical pulses. *Opt. Lett.* **1990**, *15*, 1282–1284.
61. Minardi, S.; Eilenberger, F.; Kartashov, Y.V.; et al. Three-dimensional light bullets in arrays of waveguides. *Phys. Rev. Lett.* **2010**, *105*, 263901.
62. Eilenberger, F.; Prater, K.; Minardi, S.; et al. Observation of discrete, vortex light bullets. *Phys. Rev. X* **2013**, *3*, 041031.